# Intracrystalline mesoporosity over Y zeolites. Processing of VGO and resid-VGO mixtures in FCC

Juan Rafael García, Marisa Falco, Ulises Sedran*

Instituto de Investigaciones en Catálisis y Petroquímica INCAPE
(UNL – CONICET). Colectora Ruta Nac. 168 km 0 – Paraje el Pozo
(3000) Santa Fe, Argentina.
Tel.: +54 (342) 451-1370 #6102
jgarcia@fiq.unl.edu.ar, mfalco@fiq.unl.edu.ar, usedran@fiq.unl.edu.ar*

* Corresponding author.

**Abstract**

Prototypes of FCC catalysts containing 30 %wt. Y zeolite with different intracrystalline mesoporosity generated by alkaline desilication, on an inert silica matrix, were tested in cracking a conventional vacuum gasoil (VGO) feedstock, alone and mixed with an atmospheric tower residue (ATR). The experiments were performed in a fluidized bed CREC Riser Simulator reactor (reaction time: 5-30 s, temperature: 550 °C, catalyst/feedstock: 4.5). Independently of the catalyst, the conversions of the ATR-VGO mixture were higher than those of the VGO at the same conditions. With both feedstocks, the catalyst including the zeolite with increased intracrystalline mesoporosity and higher acidity showed a higher observed activity than the catalyst with the parent zeolite. In addition, the catalyst with the modified zeolite showed higher selectivity to LCO, which is an intermediate product in FCC and a contributor to the diesel pool, especially with the ATR-VGO mixture. This effect was the consequence of the enhanced diffusion transport of primary product molecules in the zeolite pore system which, in diffusing faster, have fewer chances to be further cracked. The catalyst with higher mesoporosity showed higher coke selectivity, coke being less condensed, due to the higher free volume in the porous system allowing accommodate precursors of coke.

**Keywords:** Intracrystalline mesoporosity, Catalytic cracking, Y zeolite, Diffusion inhibitions, Resids, Fuels.

## 1. Introduction

In different refining schemes, fluid catalytic cracking (FCC) is a profitable process aimed at converting low-cost vacuum gasoil (VGO) and various heavy hydrocarbon cuts, from separation or thermal cracking processes, into valuable products [1]. Among the transportations fuels produced by the FCC process, gasoline is the main product ($C_5$-$C_{12}$ hydrocarbons, approximately 20-216 ºC boiling range), but also a middle distillate fraction (light cycle oil (LCO), $C_{12}$-$C_{20}$ hydrocarbons boiling in the 216-344 ºC range) is used in diesel blending. Moreover, important amounts of gaseous products (dry gases (DG, $C_1$-$C_2$), and liquefied petroleum gas (LPG, $C_3$-$C_4$)) are produced, which contribute to satisfy the light olefins demand as petrochemical raw materials, particularly propylene [2].

Commercial FCC catalysts are composed by Y zeolite crystals supported on a matrix, either active or inactive, while binder, filler and additives with different roles are also included [3,4]. The average particle size of the catalysts is about 70 μm, the zeolite crystals being smaller than 1 μm [4]. It is necessary that reactant molecules diffuse through the porous system of the catalyst particles in order to reach the active sites, which are mainly located in the zeolite micropore structure, adsorb and react. Then, chemical (mainly acidity) and textural properties have a controlling impact on the performance of these catalysts. Bulky molecules larger than the micropore size in Y zeolite (7.4 Å), which are typical in FCC feedstocks, would hardly access internal sites, due to serious diffusion restrictions in the pore system [3,5,6]. However, these molecules could crack on the matrix, if active, or in the external surface of zeolite crystals and thus their products would diffuse more easily in the micropores.

In the last decades, the steady decrease in the average quality of crude oils and fuel oil demand, as well as the constant fluctuations in their price stimulate the use of residual hydrocarbon cuts, such as atmospheric tower bottoms (ATR), deasphalted oil or aromatic extracts in FCC units, which are added to the conventional feedstocks [7,8].

Heavy residues are characterized by high density, viscosity and molecular weight, and low atomic hydrogen to carbon ratio [9]. Resids also differ from standard VGO feedstocks in their higher contents of contaminant metals (such as Ni, V, Na and Fe), polynuclear aromatic compounds, heteroatoms and complex macromolecular groups [10,11]. Consequently, resids have a large Conradson carbon residue (CCR), which translates into a high coking potential, which might compromise the delicate heat balance in FCC units. Other problems are that Ni contributes to increase coke and hydrogen yields, while V attacks the zeolite component in the catalyst [8]. Moreover, additional S and N in the feedstocks increase SOx and NOx emissions and the concentration of sulfur compounds among products.

One of the main challenges in the last decades in FCC is contributing more efficiently to the satisfaction of the increasing consumption of diesel fuels [12-14]. In that sense, besides a proper performance in the processing of increasingly heavier hydrocarbon feedstocks, good LCO selectivity in the catalysts is desirable [5,14,15]. High quality diesel fuels should obey rigorous specifications including distillation properties, sulfur content and cetane number. This last property is negatively affected by the concentration of aromatic species, which is particularly high in LCO [12,13,15]; nevertheless, the high LCO yields in FCC drive the upgrading of its blending quality. Since LCO is an intermediate product in the conversion scheme of FCC [5,8,16], one of the challenges in the development of novel catalysts to increase mid-distillate yields is avoiding the undesirable secondary reactions that consume LCO to produce lighter products [5].

Commercial catalysts were developed to process resids, which are particularly efficient in converting these highly demanding feedstocks. These catalysts should satisfy a number of conditions, among which high hydrothermal stability, high contaminant metal resistance, good coke selectivity and low intraparticle mass transfer limitations can be mentioned [17]. Different approaches were proposed to improve diffusion transport properties in zeolites [18]. Zeolites with extra-large pores have topologies that are different from that of Y zeolite and show lower hydrothermal stability [19]. Smaller Y zeolite crystal sizes are potentially useful [3], but they are difficult to handle and process. Oppositely, intracrystalline mesopores can be induced in

the zeolites, that is, cracks, cavities [20] and cylindrical channels [21] which are interconnected in a wormhole-like manner [18]. Among the various methods which can produce mesopores in the zeolite crystals [18,22,23], desilication has been extensively used in Y zeolite [5,6,24-27]. The method consists in selectively removing silicon atoms from the zeolite crystalline network by means of a controlled lixiviation with an alkaline agent, which produces a partial destruction of the network, thus generating mesoporosity [18].

Diffusion restrictions in porous catalysts where complex reactions take place (case of FCC) will not only impact on the observed catalyst activity but also on the selectivities to the various products [22,23,28]. In effect, it has recently been shown that FCC catalyst prototypes which were prepared with zeolites having different degrees of intracrystalline mesoporosity showed improved observed activity in the cracking of 1,3,5-tri-isopropylbenzene (critical diameter 9.5 Å), given the enhanced diffusion of the bulky reactant molecules. Moreover, the selectivity to bulky primary cracking products (di-isopropylbenzenes) was increased, due to their faster diffusion through the catalyst pore system and consequent shorter residence time, which allows avoiding secondary reactions [6]. Thus, improvements in the transport properties of commercial FCC catalysts would be attractive, because the accessibility of bulky molecules in the feedstocks could be enhanced and the selectivity to valuable intermediate products, such as diesel contributing LCO, increased by attenuating undesired secondary reactions (overcracking) [5,22,23].

In view of the need to process residual feedstocks in FCC and increase the mid-distillates yield, which require catalysts with improved transport properties, it is the objective of this work to evaluate the performance of prototype catalysts formulated with Y zeolites having different degrees of intracrystalline mesoporosity, induced by alkaline desilication, in the catalytic cracking of a conventional VGO feedstock, alone and mixed with atmospheric tower bottoms.

## 2. Experimental

### *2.1. Y zeolite desilication (alkaline leaching)*

A commercial ultrastable Y zeolite (CBV 760, Zeolyst) was subjected to desilication treatments in order to generate intracrystalline mesoporosity [6,24,26]. This Y zeolite, which has been previously steamed and acid-leached by the manufacturer, was chosen as departing material because it is adequate to be subjected to desilication in order to prepare novel catalysts for hydrocracking [24] and catalytic cracking [5]. Different portions of zeolite were suspended in NaOH solutions (1 g zeolite/30 mL solution) with concentrations of 0.05, 0.10 and 0.20 M, respectively. The suspensions were stirred during 15 min at 25 ºC and then neutralized using a 1.00 M HCl solution. The zeolites were ion exchanged three times using 0.50 M $NH_4Cl$ solutions (1 g zeolite/5 mL solution), thoroughly washed with deionized water, dried (110 ºC, 16 h) and calcined (550 ºC, 4 h) in order to recover the zeolites in their acid form. The samples were named Z-05, Z-10 and Z-20, according to the concentration of NaOH in the treatment solutions, and the parent (untreated) sample was named Z-00.

### *2.2. Zeolite characterization*

The X-ray diffraction patterns of the various modified zeolites were recorded in the $5° < 2\theta < 40°$ range on a Shimadzu XD-D1 diffractometer with Cu Kα radiation operating at 30 kV and 40 mA. The unit cell sizes were calculated following ASTM D-3942 standard and the crystallinities were calculated according to ASTM D-3906 standard using zeolite Z-00 as a reference sample, which was assigned 100 % crystallinity.

The textural properties were assessed after nitrogen adsorption at -196 °C in a Quantachrome Autosorb-1 sorptometer, the samples being previously degassed at 300 ºC during 3 h. The specific surface areas were measured according to the Brunauer-Emmett-Teller (BET) method in the $0.15 < P/Po < 0.30$ range and the total pore volumes were estimated at P/Po ~ 0.98. The micropore volumes and the specific surface areas of the mesopores were calculated with the *t*-plot method in the 3.5 Å < *t* < 5.0 Å

range. The mesopore size distributions were determined with the Barrett-Joyner-Halenda (BJH) model.

The nature, amount and strength of the surface acid sites were determined by infrared spectroscopy analysis in a Shimadzu FTIR Prestige-21 equipment using pyridine as a probe molecule. Self-supporting wafers with a density of 440 g/m$^2$ were formed by pressing approximately 100 mg of zeolite at 1 ton/cm$^2$, which were then placed into a cell with $CaF_2$ windows. Samples were initially outgassed at 450 ºC and a pressure of $10^{-4}$ Torr during 2 h, and a background spectrum was recorded after cooling down to room temperature. The adsorption of pyridine (Merck, 99.5%) was performed at room temperature and, after successive desorptions (150, 300 and 400 ºC), spectra were recorded at room temperature and a pressure of $10^{-4}$ Torr with a resolution of 4 cm$^{-1}$. The integrated absorbance of the bands at 1545 and 1450-1460 cm$^{-1}$ were used to calculate the amounts of Brönsted and Lewis acid sites, respectively, by means of the integrated molar extinction coefficients, which are considered independent from the solid composition and the acid site strength [29].

*2.3. Catalytic tests*

In order to evaluate the catalytic performances of the different zeolites in a fluidized bed reactor, prototypes of FCC catalysts were prepared. The various zeolites were steamed (100 % steam) at 788 °C during 5 h in order to stabilize them. The steamed samples were named Z-00-S, Z-05-S, Z-10-S and Z-20-S, in accordance with the nomenclature of the parent zeolites. The prototypes of FCC catalysts were formulated by mixing the stabilized zeolites (30 %wt.) with an essentially inactive matrix (50 %wt., silica gel 60, Merck, Code number 107734) and a colloidal silica binder (20 %wt., Ludox AS-40, Aldrich), thus reproducing typical formulations of commercial FCC catalysts [3,4]. Once calcined (550 ºC, 4 h), the catalysts were ground and sieved, and the 75-125 μm fraction was used. The catalysts were designated as Cat-00, Cat-05, Cat-10 and Cat-20, according to the nomenclature of the corresponding zeolites.

The conversion experiments were performed in a CREC Riser Simulator reactor, a batch fluidized bed laboratory unit with internal recirculation, which closely mimics the conditions of the commercial FCC process [30]. This reactor was specifically designed for FCC studies, and a comprehensive additional description can be found elsewhere [3,15,30,31]. The catalytic evaluation was performed using two feedstocks: a) a conventional FCC VGO, and b) a mixture of the VGO with 10 %wt. of an atmospheric tower residue ATR. The properties of both the VGO and the ATR cuts are shown in Table 1. Reaction times in the experiments ranged from 5 to 30 s, the reaction temperature was 550 °C and the catalyst to oil relationship was 4.5, achieved with a mass of catalyst of 0.6 g in all the cases. The reaction products were analyzed on-line by conventional capillary gas chromatography, using a 30 m long, 250 μm diameter and 0.25 μm film thickness, non-polar, dimethylpolysiloxane column. Coke content on the catalyst was assessed by burning-off the carbonaceous materials following a temperature programmed oxidation method, further methanation of the carbon oxides formed over a Ni catalyst, and quantification of methane with the help of a FID detector. Mass balances (recoveries) in all the experiments closed to more than 90 %.

**Table 1**. Properties of the VGO and ATR feedstocks.

| | VGO | ATR |
|---|---|---|
| Density 20/4 ºC (g/cm$^3$) | 0.9162 | 0.9370 |
| º API | 22.94 | 19.51 |
| CCR (% wt.) [a] | 0.11 | 14.8 |
| Distillation curve (ºC) [b] | | |
| Initial | 199 | 240 |
| 10 % vol. | 345 | 347 |
| 30 % vol. | 405 | 432 |
| 50 % vol. | 438 | 483 |
| 70 % vol. | 465 | 538 |
| 90 % vol. | 495 | |
| Final | 512 | |
| Nickel (ppm) | 0.10 | 0.83 |
| Vanadium (ppm) | 0.73 | 2.1 |
| Sodium (ppm) | 0.38 | 8.1 |
| Iron (ppm) | 2.36 | 4.0 |
| Copper (ppm) | < 0.02 | 0.05 |
| Sulphur (% wt.) | 0.39 | 0.19 |
| SARA fractions (% wt.) [c] | | |
| Saturated | 68 | 52 |
| Aromatics | 20 | 10 |
| Resins | 11 | 24 |
| Asphaltenes | 1 | 13 |

a- ASTM D-4530.

b- ASTM D-1160.

c- ASTM D-2007.

## 3. Results and discussion

### *3.1. Physicochemical properties*

Table 2 shows the textural and crystalline properties of the parent and modified zeolites. A more detailed discussion about the Y zeolite desilication process and its impact on the zeolite properties, which are out of the scope of this work, can be found elsewhere [5,6,18,25,26]. However, given the fact that the performances of the catalysts in converting actual FCC feedstocks will be conditioned by their physical (textural) and chemical (mainly acidity) properties, it is important to point out the most important modifications in the zeolites after the alkaline treatment.

**Table 2**. Textural and crystalline properties of the parent zeolite and desilicated samples.

| | Z-00 | Z-05 | Z-10 | Z-20 |
|---|---|---|---|---|
| Textural properties | | | | |
| BET specific surface area ($m^2/g$) | 838 | 835 | 828 | 724 |
| Micropore specific surface area ($m^2/g$) [a] | 612 | 477 | 462 | 270 |
| Mesopore specific surface area ($m^2/g$) | 226 | 358 | 366 | 454 |
| Total pore volume ($cm^3/g$) | 0.632 | 0.659 | 0.686 | 0.810 |
| Micropore volume ($cm^3/g$) | 0.350 | 0.272 | 0.266 | 0.158 |
| Mesopore volume ($cm^3/g$) [a] | 0.282 | 0.387 | 0.420 | 0.652 |
| Average mesopore diameter (Å) | 28.7 | 28.2 | 44.2 | 56.2 |
| Crystalline properties | | | | |
| Crystallinity (%) | 100 [b] | 75 | 66 | 54 |
| Unit cell size (Å) | 24.23 | 24.24 | 24.25 | 24.26 |

a- Micropore surface area = BET specific surface area – Mesopore surface area.
Mesopore volume = Total pore volume – Micropore volume.

b- Reference sample.

It can be seen that the higher the NaOH concentration in the solutions, the higher the increase in mesoporosity. This reflects on both the mesopore specific surface area, which increases up to two times the initial value in the case of sample Z-20, and the mesopore volume. The increase in mesoporosity was in all the cases produced together

with a loss in microporosity, which was more pronounced when the alkaline treatment was more severe. Pore size distributions (not shown) suggested that the new mesopores correspond to the 20 - 300 Å range [6]. Moreover, their average sizes also increased following the severity of the treatments.

The X-ray diffraction analysis showed that the loss of crystallinity in the zeolite followed the concentration of the alkaline solutions. For example, in the case of the highest NaOH concentration, 0.20 M, the resulting crystallinity in the desilicated zeolite was only half the crystallinity of the parent zeolite. A similar behaviour was reported by Verboekend et al. [25], in the alkaline leaching of the same type of zeolite, which was attributed to the partial destruction of the framework after the removal of Si atoms (desilication) [18,25]. The sizes of the unit cells increased slightly with the desilication treatment, as a consequence of the selective silicon extraction, since the length of Si-O bonds in the zeolite framework is shorter than that of the Al-O bonds, thus producing a larger unit cell sizes [4]. But, in general, UCSs were overall small, in the 24.23 to 24.26 Å range.

Fig. 1 shows the distributions of acid sites in the parent and modified zeolites according to their strength, as determined by FTIR analysis of adsorbed pyridine (all the zeolites were in their protonic form). It can be seen that the amount of acidic sites in a mass basis increased in the zeolites after the alkaline lixiviation and ion exchange steps. The alkaline process is highly selective in leaching silica-rich domains [18]. Therefore, the aluminum-rich domains would remain relatively unchanged, thus producing enrichment in Al tetrahedron atoms and, consequently, an increase in acidity. This process was observed especially in zeolites Z-05 and Z-10, which did not suffer a severe loss of crystallinity, differently from zeolite Z-20, which showed more important loss of crystallinity and, therefore, its increase in acidity was smaller than that of sample Z-10. Then, for the range of concentrations of alkali used in this series, there is an optimum concentration of NaOH in reference to the zeolite's acidic property. Even though alkaline leaching is highly selective to silicon removal, experimental evidences exist which demonstrate that a certain amount of aluminum is removed as well during the mesopores formation mechanism [25,27]. Then, these dissolved species can be partially

reincorporated as silica-alumina extraframework species, which can contribute a certain degree of acidity, especially Lewis-type, to the solid [27,32].

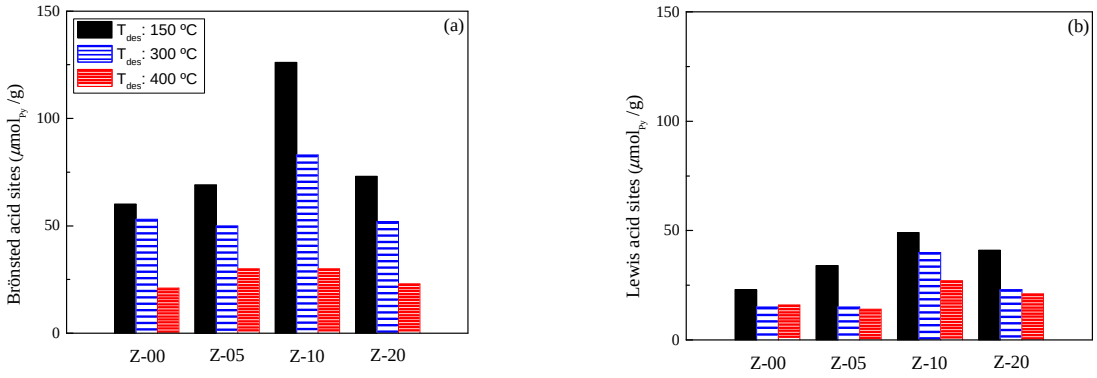


**Fig. 1.** Distribution of (a) Brönsted and (b) Lewis acid sites in the parent and desilicated zeolites (pyridine FTIR).

In order to perform the catalytic evaluation of parent and modified zeolites in a fluidized bed reactor, prototypes of FCC catalysts were prepared as described in Section 2.3. It is necessary to steam the zeolites before the preparation of the compound catalysts (zeolite plus matrix and binder) in order to mimic the hydrothermal stabilization produced in commercial units [3-5]. The properties of steamed zeolites are shown in Tables S1 and S2 (Supplementary File). Steaming the zeolites led to expected results; that is, there was a loss of specific surface area and crystallinity, which was more severe on the desilicated samples. The acidity of the different samples also decreased after steaming. However, all the properties (specific surface area, average mesopore size, crystallinity, acidity) maintained the relative magnitudes that had been observed with the zeolites before steaming. This behavior is consistent with previous observations from Martinez and co-workers [5], who studied the hydrothermal stabilization of Y zeolites subjected to different post-synthesis modifications.

Even though the silica used as the matrix could contribute some mesoporous surface area to the compound catalyst, previous studies showed that its contribution to the overall catalytic activity is essentially nil [15]. In this manner, both the catalytic activity and the major diffusion restrictions in the compound catalysts can be attributed

to the zeolitic component. The textural properties of the compound catalysts are shown in Table S3 (Supplementary File). It can be seen that the micropore specific surface area of prototype Cat-00 was slightly higher than that of catalyst Cat-10, in accordance with the properties of their parental zeolites.

### *3.2. Catalytic tests*

#### *3.2.1 Activity*

The catalytic performance of the complete catalyst series was evaluated recently by means of the catalytic cracking of the model compound 1,3,5-tri-isopropylbenzene (TIPB, critical diameter 9.5 Å) [6]. TIPB was the choice in the study of diffusion-reaction phenomena not only because of its molecular size, which is significantly larger than the pore size of Y zeolite (7.4 Å), but also because its reaction can be tracked relatively easily. In effect, the TIPB cracking reaction follows a sequential path of the scissions of the side alkyl chains, while the aromatic ring keeps essentially unaltered [3]. This sequential scheme (1,3,5-tri-isopropylbenzene → 1,3-di-isopropylbenzene → cumene → benzene) allows observing product distributions under a kinetic approach which considers the influence of diffusion restrictions on primary and secondary cracking reactions [6].

Fig. 2 shows the TIPB conversion as a function of reaction time over the various catalysts at 500 °C and cat/oil 4.7. These results show that all the catalysts prepared with the modified zeolites with increased intracrystalline mesoporosity were more active than that prepared with the parent zeolite. Moreover, the higher the intracrystalline mesoporosity, the higher the selectivity to the primary cracking product in the series mechanism (1,3-di-isopropylbenzene) and the lower the selectivity to the secondary cracking products (cumene and benzene). The higher observed activity was the consequence of both the higher intracrystalline mesoporosity (see Table 2), which increases the accessibility of bulky TIPB molecules to the active sites, and the higher density of acid sites (see Fig. 1), which catalyse the cracking reactions. Then, catalyst Cat-10 was the most active in the series, given the zeolite Z-10 provided an important mesoporosity and the highest acidity. As it was shown in Fig. 1, zeolites Z-05 and Z-20

have similar acidities; then, the difference in the activity of catalysts Cat-05 and Cat-20 can be assigned to the higher intracrystalline mesoporosity in zeolite Z-20 as compared to Z-05 (refer to Table 2). Independently from the acid property, the existence of intracrystalline mesoporosity in the zeolitic component of the catalysts improves the cracking of bulky molecules and favours the selectivity to bulky intermediate products which, in diffusing faster out of the zeolite porous system, are less prone to secondary reactions [6,28].

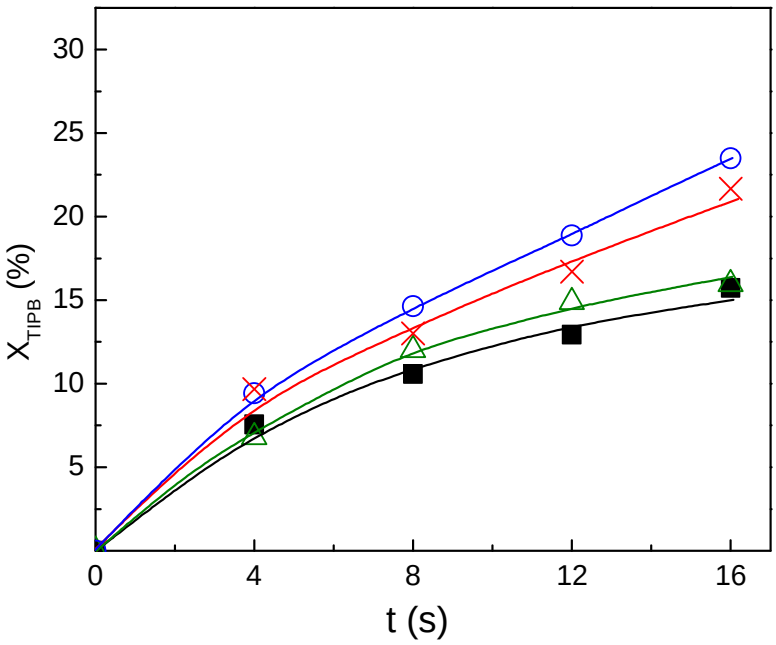


**Fig. 2.** Conversion of 1,3,5-tri-isopropylbenzene at 500 °C over the parent and the desilicated zeolites. Symbols: *square* Cat-00; *triangle* Cat-05; *circle* Cat-10; *cross mark* Cat -20. Reproduced from Ref. [6] with permission of Springer.

Given these evidences about the superior performance of the catalysts formulated with desilicated zeolites in the cracking of a model molecule, catalyst Cat-10, containing the zeolite desilicated with NaOH 0.10 M solution, in turn the most active in the series, was chosen to be compared against the parent catalyst in the processing of actual refinery feedstocks. A typical VGO was the reference, and a mixture with 10 % ATR was assumed a realistic representation of resid co-processing operations.

It can be seen in Fig. 3 that the conversion profiles of the VGO and ATR-VGO mixture over both Cat-00 and Cat-10 catalysts are increasing as a function of reaction time, being steeper at short times, as expected in a batch reactor [31]. Moreover, this is the common behaviour in FCC units as a function of position in the riser reactors [8]. Note that the conversions achieved with these prototypes are similar to the typical values in commercial equilibrium catalysts [17].

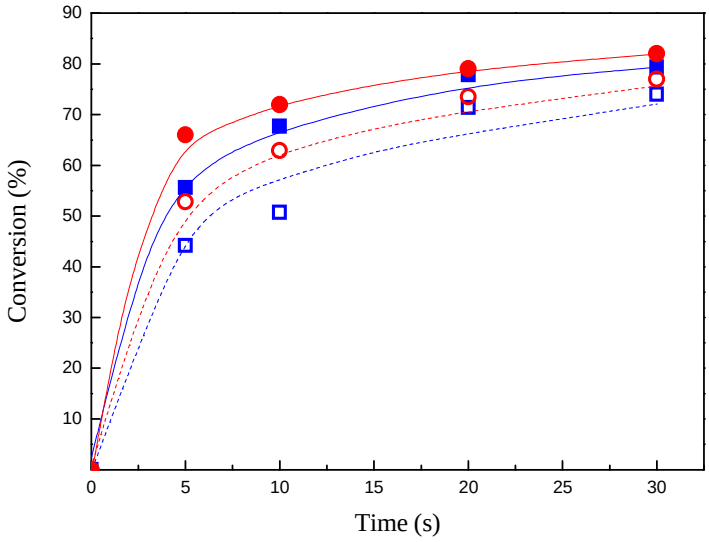


**Fig. 3.** Conversion of pure VGO (open symbols, dashed lines) and ATR-VGO mixture (closed symbols, full lines) feedstocks over catalyst Cat-00 (■) and Cat-10 (●) as a function of time.

It can be observed that, independently of the catalyst, the conversions of the ATR-VGO mixture were higher than those of the VGO alone. The same behaviour had been observed in experiments with equilibrium commercial FCC catalysts [17]. The differences in the conversion profiles could be the consequence of the higher reactivity of the residual fraction as compared to VGO [17,33]. In effect, some hydrocarbon molecules with high molecular weight in the resid fraction could have aromatic rings in their nuclei and long aliphatic side chains, which could be even longer than those in the VGO feedstock [11,14]. These aliphatic chains would behave in FCC in a way similar to a more paraffinic feedstock, which is expected to be more crackable [14].

In comparing the performances of the two catalysts, it can be observed in Fig. 3, with both feedstocks, that catalyst Cat-10, with higher intracrystalline mesoporosity, was more active than the base catalyst Cat-00. The higher activity of catalyst Cat-10 is consistent with previous experiments with hydrocarbon model compounds such as TIPB [6] and *n*-hexadecane [34] and bio-oil from wood sawdust, which is a very complex mixture of oxigenated compounds, some of them with bulky molecules [26]. The same concepts as those used to rationalize the results of TIPB conversion shown in Fig. 2 can be used in all the other cases.

*3.2.2 Product distributions*

Fig. 4 shows the yield curves of the various hydrocarbon cuts typical in FCC which were observed in the conversion of VGO and ATR-VGO feedstocks over both catalysts. It can be seen that at conversions close to 75 %, yields are in the usual ranges reported for the conversion of commercial feedstocks at similar conditions in fluidized bed reactors [1,31,33]. In general terms, independently from the feedstock and the catalyst, gasoline and LCO are the products with the highest yields. Moreover, in all the cases, the yield of LCO shows a maximum as a function of the conversion, which indicates its well-known intermediate role in the overall conversion mechanism in FCC [8]. Gasoline and gas yields are steadily increasing as a function of conversion.

When catalyst Cat-00 was used, only minimum differences were observed in the yield curves from both feedstocks (see Fig. 4a). That was not the case when the catalyst with higher intracrystalline mesoporosity was employed (Cat-10, Fig. 4b), where the yield curves were somewhat different for each feedstock. This is also reflected in Table 3, where selectivities and some product quality indexes are shown.

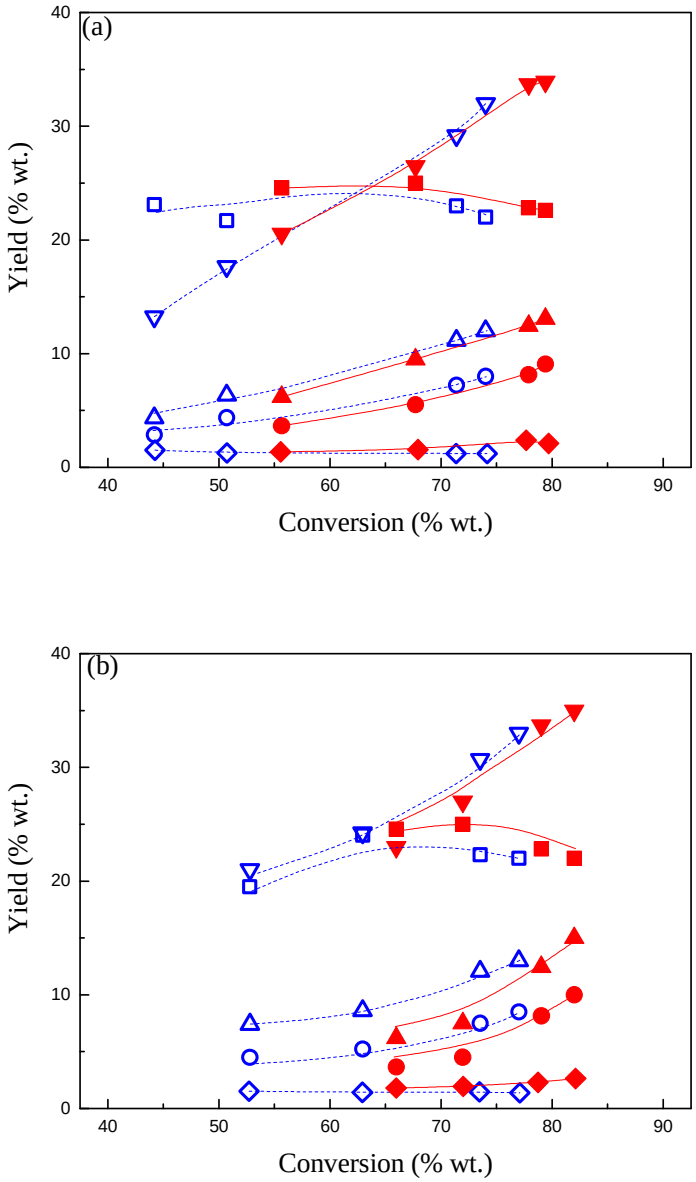


Fig. 4. Hydrocarbon yields as a function of the conversion of VGO and ATR-VGO resid feedstock over catalysts (a) Cat-00 and (b) Cat-10. Symbols: open, dashed lines (VGO); close, full lines (ATR-VGO); dry gases (●); LPG (▲); gasoline (▼); LCO (■); coke (♦).

It can be seen in Table 3 that catalyst Cat-10 produced selectively less gases than catalyst Cat-00, this difference being more significant when ATR is added to VGO conventional feedstock. The lower gas selectivity was also reported by García-Martínez et al. [22], who used mesostructured Y zeolites in cracking VGO. They concluded that mesopores would facilitate diffusion transport of the feed and the product molecules

into and out of the zeolite pore system, thus reducing the secondary reactions, such as gasoline and LCO overcracking to yield gases [22]. Moreover, it can be seen with both feedstocks that catalyst Cat-10 produced $C_4^=$ / $C_4$ *total* relationships which were lower than those in catalyst Cat-00, this being more noticeable when the ATR-VGO mixture was the feedstock. This index has been used as an indicator of the magnitude of hydrogen transfer reactions: the lower the relationship, the more intense the reactions, which consume olefins [35-37]. Then, the $C_4^=$ / $C_4$ *total* values shown in Table 3 indicate a higher incidence of hydrogen transfer reactions in catalyst Cat-10, which can be attributed to its higher density of acidic sites (see Fig. 1), hydrogen transfer reactions depending on paired acid sites [38]. This same comparative analysis can be performed with the $C_5^=$ / $C_5$ *total* relationship in the gasoline cut, which has also been used as an index to quantify hydrogen transfer [35].

**Table 3.** Selectivities and quality indexes indices of the various cuts (Conversion approximately 75 % wt.).

| | **VGO** | | **ATR-VGO** | |
|---|---|---|---|---|
| | **Cat-00** | **Cat-10** | **Cat-00** | **Cat-10** |
| $S_{DG}$ (% wt.) | 10.6 | 9.9 | 10.3 | 6.8 |
| $S_{LPG}$ (% wt.) | 16.0 | 16.0 | 15.6 | 11.4 |
| $C_4^=$ / $C_4$ *total* | 0.88 | 0.86 | 0.84 | 0.71 |
| $S_{gasoline}$ (% wt.) | 42.5 | 40.9 | 42.4 | 41.1 |
| $C_5^=$ / $C_5$ *total* | 0.74 | 0.72 | 0.71 | 0.53 |
| Arom $C_{10}$ / gasoline (% wt.) | 8.00 | 7.09 | 6.64 | 6.01 |
| Arom $C_{11}$ / gasoline (% wt.) | 0.55 | 0.52 | 0.53 | 0.48 |
| $S_{LCO}$ (% wt.) | 29.3 | 30.9 | 29.6 | 38.1 |
| Arom $C_{12}$ / LCO (% wt.) | 6.0 | 5.4 | 6.1 | 4.9 |
| Arom $C_{13}$ / LCO (% wt.) | 4.5 | 4.0 | 3.8 | 2.9 |
| Arom $C_{14}$ / LCO (% wt.) | 8.0 | 6.5 | 6.7 | 5.4 |
| Arom $C_{15}$ / LCO (% wt.) | 0.7 | 1.8 | 1.7 | 0.8 |
| Arom $C_{16}$ / LCO (% wt.) | 3.1 | 1.9 | 1.9 | 2.1 |
| $S_{coke}$ (% wt.) | 1.6 | 2.5 | 2.1 | 2.6 |

Concerning gasoline, the selectivities observed when processing both feedstocks were very similar (42.5% wt. for Cat-00, and 41% wt. for Cat-10). In the case of LCO, a slightly higher selectivity was observed with catalyst Cat-10 when VGO was processed alone. However, when ATR was added to VGO, differences between catalysts were more important. In effect, when the catalyst with the higher intracrystalline mesoporosity and acidity (Cat-10) was used, the lower selectivity to gasoline (-1.3 percentage points as compared to VGO alone) was compensated by the much higher selectivity to LCO (+8.5 percentage points) as compared to the base catalyst (Cat-00). The higher yield of LCO produced by catalyst Cat-10 is the consequence of the improvements in the diffusion processes of bulky molecules in the range of LCO. The higher selectivity to LCO was also observed by García-Martínez et al. [22] in the cracking of VGO, who used mesostructured Y zeolites prepared through a surfactant templating approach. They stated that the mesopores would facilitate the transport of molecules in the zeolite crystals, thereby reducing undesirable secondary reactions. Moreover, it has also been postulated that extraframework silica-alumina species could be formed during the alkaline leaching and later neutralization steps in zeolite desilication [6,27,32]. Those amorphous species could behave as cracking active sites converting large molecules to LCO more selectively [39]. As already mentioned, LCO can be considered an intermediate product in the conversion scheme of FCC and, consequently, in diffusing faster out of the pore system, its molecules will be less subjected to additional cracking reactions leading to lighter products [5,8,22]. This effect seems to overwhelm the higher acidity of zeolite Z-10, which would be expected to produce a higher degree of advancement towards lighter products in the mechanism of consecutive reactions [8,15].

As already mentioned, the LCO cut from FCC can be used as a contributor to the diesel pool, but its composition, which includes very high proportions of aromatic hydrocarbons, is a negative factor [12,13]. Table 3 includes the selectivities to aromatic hydrocarbons in LCO and heavy gasoline range, according to the number of carbon atoms per molecule. It can be seen in general terms that, whichever the catalyst, the selectivities to aromatics in LCO were lower when the feedstock was the ATR-VGO mixture. Independently from the feedstock, the proportion of aromatic hydrocarbons in LCO produced by catalyst Cat-10 was lower than that of catalyst Cat-00. A simple

conversion scheme in FCC would indicate that the naphthenic and paraffinic compounds can be converted into olefins and paraffins and, in turn, the naphthenics compounds into aromatics [16]. But, essentially, aromatics produce aromatics and coke, with the exception of those including long side chains [14]. Given the more refractory character of aromatic hydrocarbons, it is to be expected that the more extended the reaction advancement, the higher the proportion of aromatics. Thus, it is to be expected that higher diffusion restrictions in the base catalyst (Cat-00), which lead to longer residence times in its porous system, would allow a greater occurrence of side reactions, leading to a higher selectivity of aromatics, as compared to the modified catalyst (Cat-10) [5]. In fact, based on large databases, it has been postulated that high accessibility FCC catalysts would show lower promotion of hydrogen transfer reactions, which lead to aromatics formation, than low accessibility catalysts [17]. The dilution of aromatics with other hydrocarbons, due to the noticeably higher LCO yield, is another factor which could contribute to the lower aromatics concentration in the heavy gasoline and LCO ranges when the ATR-VGO was processed [11,14,17,33], especially when the modified catalyst (Cat-10) was used.

*3.2.3 Coke*

The additional coke yield expected when a resid is co-processed together with VGO in the FCC deserves particular consideration, since it could contribute to threaten the delicate energetic balance in commercial units [33]. Consistently, as it can be seen in Table 3, the coke selectivity was higher over both catalysts when ATR was added to VGO. This is expected, since the ATR has a higher coke forming potential, as suggested by its higher CCR index (see Table 1). Moreover, it can be seen that independently of the feedstock, the coke selectivity was higher in catalyst Cat-10 than in the base catalyst Cat-00. It has been postulated that in the initial steps of coke formation in zeolites, precursor molecules originate in the cages and then overflow to the external surface of the crystal [40,41], or, in the case of intracrystalline mesopores, coke would pour out towards mesopores in the crystals. This increased tendency to form coke in the catalyst with intracrystalline mesoporosity had been observed previously in the catalytic processing of pine [26,42] and maple [43] sawdust bio-oils over zeolites with various degrees of intracrystalline mesoporosity, which was attributed to the existence of more

free volume in the porous system allowing the polymerization of coke precursor compounds.

Fig. 5 shows the coke combustion profiles of both catalysts after processing VGO and ATR-VGO feedstocks, conversion being approximately 75 % wt. The profiles confirm the higher coke yields from the ATR-VGO mixture in comparison with VGO (see Table 3), and also confirm the higher coke selectivity in catalyst Cat-10 compared with Cat-00. It is interesting to note that whichever the feedstock, the peak maxima are located at lower temperatures in the case of catalyst Cat-10. For example, coke from VGO showed maxima at 645 ºC with catalyst Cat-00 and 623 ºC with catalyst Cat-10; coke from ATR-VGO showed them at 587 and 565 ºC, respectively. It has been postulated that coke in FCC catalysts is located mostly on the matrix mesopores, or into the mesopores formed by eventual dealumination during the equilibration process, arranged into polyaromatic domains which are heterogeneously distributed and which also include trapped saturated hydrocarbon molecules [40]. An analogy could be established between the intracrystalline mesopores generated by alkaline leaching over the zeolites used in this work, and the mesopores in the matrix of commercial FCC catalysts. Thus, a higher intracrystalline mesoporosity (higher mesopore volume, see Table 2) would include a higher proportion of saturated hydrocarbon molecules, which confer coke a less condensed character. In fact, the easier coke burning-off in the regeneration step had been mentioned by Hartmann [44] for zeolites having mesopores. For both catalysts a less condensed character in coke was observed when the ATR-VGO mixture was processed, in comparison with the conventional VGO feedstock.

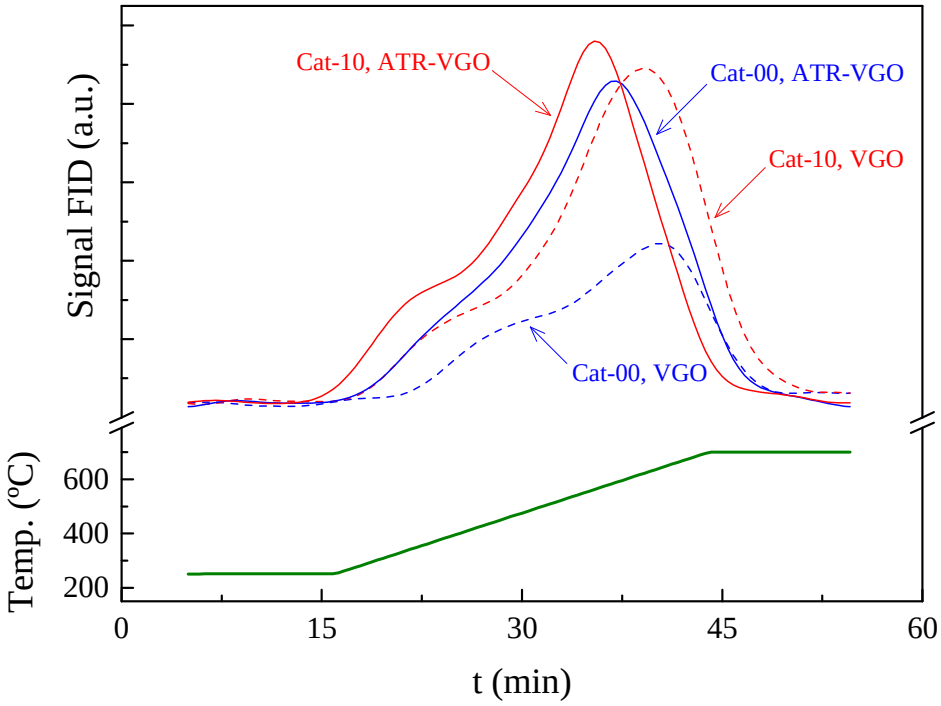


**Fig. 5.** Coke combustion (TPO) profiles for the catalysts used in the cracking of pure VGO and ATR-VGO mixture (Conversion ~ 75 % wt.).

## 4. Conclusions

The conversion of a conventional FCC feedstock (vacuum gas oil), both alone and with the addition of 10 %wt. of an atmospheric tower residue, over prototypes of FCC catalysts with Y zeolites having different degree of intracrystalline mesoporosity, was successfully performed in a CREC Riser Simulator reactor, under conditions close to those in the commercial FCC process.

Independently of the catalyst, the conversions of the ATR-VGO mixture at the same reaction conditions were higher than those of the VGO alone. With both feedstocks, the catalyst with higher intracrystalline mesoporosity showed a higher observed activity than the base catalyst. This was the consequence of the better diffusion transport of bulky molecules in the feedstock, which improves their

accessibility to the active sites, and the higher density of acid sites catalysing the cracking reactions.

With both the VGO and the ATR-VGO mixture, but particularly with the latter feedstock, the catalyst with the modified zeolite showed a higher selectivity to light cycle oil, which is an intermediate product in the conversion scheme of FCC and a contributor to the diesel pool. Despite the higher acidity of the modified catalyst, which would lead to a higher degree of advancement towards lighter products in the mechanism of consecutive cracking reactions, its higher selectivity to mid-distillates was the consequence of the improvements in the diffusion transport of primary product molecules in the zeolite pore system. In that way, diffusing faster out of the pores, those molecules have fewer chances to be subjected to further cracking.

As expected, with both catalysts, the coke selectivity in the cracking of the ATR-VGO mixture was higher than that of the VGO, since the ATR has a higher CCR index. The catalyst with higher mesoporosity showed higher coke selectivity due to the higher free volume in the porous system to accommodate coke precursors; however, the coke was less condensed.

The relative performance of these prototype catalysts in the cracking of actual FCC feedstocks (higher activity and better selectivity to intermediate products in sequential reactions for the catalyst with higher intracrystalline mesoporosity), is consistent with previous findings in the cracking of model hydrocarbon reactants (1,3,5-tri-isopropylbenzene and *n*-hexadecane) and in the catalytic upgrading of bio-oil from wood sawdust. These results suggest that the intracrystalline mesoporosity in the zeolitic component of the FCC catalysts is particularly useful to process feedstocks containing bulky molecules, especially when higher selectivities to intermediate products are desired.

**Acknowledgements**

The financial support of Universidad Nacional del Litoral (Project CAID 2011 #50120110100546) and CONICET (PIP 593/13) is gratefully acknowledged.

**References**

[1] J. Speight, The Chemistry and Technology of Petroleum, fifth ed., CRC Press-Taylor & Francis Group, Boca Raton, 2014.

[2] S. Sadrameli. Fuel 173 (2016) 285-297.

[3] S. Al-Khattaf, H. de Lasa. Appl. Catal. A 226 (2002) 139-153.

[4] J. Scherzer. Catal. Rev. Sci. Eng. 31 (1989) 215-354.

[5] C. Martinez, D. Verboekend, J. Pérez-Ramírez, A. Corma. Catal. Sci. Technol. 3 (2012) 972-981.

[6] J.R. García, M. Falco, U. Sedran. Top. Catal. 59 (2016) 268-277.

[7] U. Alkemade, S. Paloumbis. Stud. Surf. Sci. Catal. 100 (1996) 339-354.

[8] R. Harding, A. Peters, J. Nace. Appl. Catal. A 221 (2001) 389-396.

[9] M. Golmohammadi, S. Ahmadi, J. Towfighi. J. Supercrit. Fluids 113 (2016) 136-143.

[10] H. Jeon, S. Park, S. Woo. Appl. Catal. A 306 (2006) 1-7.

[11] R. Sahu, B. Song, J. Im, Y. Jeon, C. Lee. J. Ind. Eng. Chem. 27 (2015) 12-24.

[12] UOP, Diesel Fuel Specifications and Demand for the 21st Century, UOP LLC, Des Plaines, 1998.

[13] Chevron, Diesel Fuel Technical Review, Chevron Corporation, San Ramon, 2007.

[14] A. Corma, L. Sauvanaud. Stud. Surf. Sci. Catal. 166 (2007) 41-54.

[15] W. Gilbert, E. Morgado, M. de Abreu, G. de la Puente, F. Passamonti, U. Sedran. Fuel Process. Technol. 92 (2011) 2235-2240.

[16] P. O'Connor. Stud. Surf. Sci. Catal. 166 (2007) 227-251.

[17] A. Devard, G. de la Puente, F. Passamonti, U. Sedran. Appl. Catal. A 353 (2009) 223-227.

[18] K. Na, M. Choi, R. Ryoo. Microporous Mesoporous Mater. 166 (2013) 3-19.

[19] A. Corma, M. Diaz-Cabañas, J. Jordá, C. Martínez, M. Moliner. Nature 443 (2006) 842-845.

[20] A. Gayubo, A. Alonso, B. Valle, A. Aguayo, J. Bilbao. Appl. Catal. B 97 (2010) 299-306.

[21] A. Janssen, A. Koster, K. de Jong. J. Phys. Chem. B 1067 (2002) 11905-11909.

[22] J. García-Martínez, M. Johnson, J. Valla, K. Li, J. Ying. Catal. Sci. Technol. 2 (2012) 987–994.

[23] T. Prasomsri, W. Jiao, S. Weng, J. García-Martínez. Chem. Commun. 51 (2015) 8900–8911.

[24] K. de Jong, J. Zečević, H. Friedrich, P. de Jongh, M. Bulut, S. van Donk, R. Kenmogne, A. Finiels, V. Hulea, F. Fajula. Angew. Chem. Int. Ed. 49 (2010) 10074-10078.

[25] D. Verboekend, G. Vilé, J. Pérez-Ramírez. Adv. Funct. Mater. 22 (2012) 916-928.

[26] J.R. García, M. Bertero, M. Falco, U. Sedran. Appl. Catal. A 503 (2015) 1-8.

[27] V. Rac, V. Rakic, C. Stošic, O. Otman, A. Auroux. Microporous Mesoporous Mater. 194 (2014) 126–134.

[28] A. Wheeler. Adv. Catal. 3 (1951) 249-327.

[29] C. Emeis. J. Catal. 141 (1993) 347-354.

[30] H. de Lasa, Novel Riser Simulator Reactor. US Patent 5.102.628, 1992.

[31] H. de Lasa, D. Kraemer, Novel techniques for FCC catalyst selection and kinetic modelling, in: H. de Lasa, G. Doğu, A. Ravella (Eds.), Chemical Reactor Technology for Environmentally Safe Reactors and Products (NATO ASI Series E-Vol. 225), Kluwer Academic Publishers, Dordrecht, 1993, pp. 71-131.

[32] E. Hensen, D. Poduval, V. Degirmenci, D. Michel Ligthart, W. Chen, F. Maugé, M. Rigutto, J. Rob van Veen. J. Phys. Chem. C 116 (2012) 21416-21429.

[33] W. Gilbert, G. Baptista, A. Pinho. Stud. Surf. Sci. Catal. 166 (2007) 31-39.

[34] J.R. García, M. Falco, U. Sedran. Ind. Eng. Chem. Res. 56 (2017) 1416-1423.

[35] J. Scherzer, R. Ritter. Ind. Eng. Chem. Res. 17 (1978) 219-223.

[36] C. Hayward, W. Winkler. Hydroc. Process. 69 (1990) 55-56.

[37] F. Guerzoni, J. Abbot. J. Catal. 139 (1993) 289-303.

[38] G. de la Puente, U. Sedran. Chem. Eng. Sci. 55 (2000) 759-765.

[39] A. Corma, C. Martínez, L. Sauvanaud. Catal. Today 127 (2007) 3-16.

[40] H. Cerqueira, G. Caeiro, L. Costa, F. Ramôa Ribeiro. J. Molec. Catal. A: Chemical 292 (2008) 1-13.

[41] M. Guisnet, P. Magnoux, D. Martin, Stud. Surf. Sci. Catal. 111 (1997) 1-19.

[42] H. Park, H. Heo, J. Jeon, J. Kim, R. Ryoo, K. Jeong, Y. Park. Appl. Catal., B: Env. 95 (2010) 365-373.

[43] A. Foster, J. Jae, Y. Cheng, G. Huber, R. Lobo. Appl. Catal. A: Gen. 423 (2012) 154-161.

[44] M. Hartmann, Angew. Chem. Int. Ed. 43 (2004) 5880-5882.